



HAL
open science

A Device for the Simultaneous Determination of the Water Retention Properties and the Hydraulic Conductivity Function of an Unsaturated Coarse Material; Application to a Green-Roof Volcanic Substrate

Filip Stanić, Yu-Jun Cui, Pierre Delage, Emmanuel de Laure, Pierre-Antoine Versini, Daniel Schertzer, Ioulia Tchiguirinskaia

► **To cite this version:**

Filip Stanić, Yu-Jun Cui, Pierre Delage, Emmanuel de Laure, Pierre-Antoine Versini, et al.. A Device for the Simultaneous Determination of the Water Retention Properties and the Hydraulic Conductivity Function of an Unsaturated Coarse Material; Application to a Green-Roof Volcanic Substrate. *Geotechnical Testing Journal*, 2019, 43 (3), pp.20170443. 10.1520/GTJ20170443 . hal-03045911

HAL Id: hal-03045911

<https://enpc.hal.science/hal-03045911v1>

Submitted on 7 Jul 2023

HAL is a multi-disciplinary open access archive for the deposit and dissemination of scientific research documents, whether they are published or not. The documents may come from teaching and research institutions in France or abroad, or from public or private research centers.

L'archive ouverte pluridisciplinaire **HAL**, est destinée au dépôt et à la diffusion de documents scientifiques de niveau recherche, publiés ou non, émanant des établissements d'enseignement et de recherche français ou étrangers, des laboratoires publics ou privés.

1 A device for the simultaneous determination of the water retention properties and
2 the hydraulic conductivity function of an unsaturated coarse material; application to
3 a green-roof volcanic substrate

4
5 Filip STANIĆ^{1,2}, Yu-Jun CUI¹, Pierre DELAGE¹, Emmanuel DE LAURE¹, Pierre-Antoine
6 VERSINI², Daniel SCHERTZER², Ioulia TCHIGUIRINSKAIA²

7 ¹ Ecole des Ponts ParisTech, Navier/CERMES, Marne la Vallée, France

8 ² Ecole des Ponts ParisTech, HM&Co, Marne la Vallée, France

9

10

11

12

13

14 Corresponding author:

15 Prof. Pierre Delage

16 Ecole des Ponts ParisTech

17 6-8 av. Blaise Pascal, Cité Descartes, Champs-sur-Marne

18 77455 Marne-la-Vallée cedex 2

19 France

20

21 Email: pierre.delage@enpc.fr

22 Phone: +33 1 64 15 35 50

23 Fax: +33 1 64 15 35 6

24 **Abstract**

25 The determination of the water retention curve (WRC) and the hydraulic conductivity function
26 (HCF) of a specific volcanic coarse granular material used as a substrate for urban green roofs in
27 Europe was carried out on a newly developed specific device in which low suctions, typical of
28 coarse granular materials, were controlled. Smaller suctions (up to 32 *kPa*) were imposed by
29 using a hanging column system and larger suctions (between 32 and 50 *kPa*) were imposed by
30 using the axis translation technique in the same cell. The changes in suction during the tests were
31 monitored by using a high accuracy differential pressure transducer. They were also used to
32 determine the hydraulic conductivity function by means of both **Kunze and Kirkham** and
33 Gardner's method. **The former technique was used at low suctions (< 4 *kPa*) to account for the**
34 **impedance effects due to the high air entry value ceramic porous disk and the latter was used**
35 **between 4 and 50 *kPa*.** Good comparability was observed in the data from both methods,
36 demonstrating the good performance of the device. **The mathematical expressions of the water**
37 **retention curve of van Genuchten and Brooks and Corey were used, and a good fitting with our**
38 **experimental data was obtained. Conversely, the hydraulic conductivity functions derived from**
39 **these expressions appeared to lead to a significant under-estimation, confirming the need of**
40 **operational and simple device for the experimental determination of the HCF.** Also, this material
41 proved to be an appropriate material for green urban infrastructures, due to light weight,
42 **satisfactory water retention capability** and hydraulic conductivity.

43
44 Key words: Green-roof material; water retention; hydraulic conductivity; hanging column; axis
45 translation; Gardner's method; Kunze and Kirkham's method

46

47 1. Introduction

48 Within the context of global warming, green roofs are considered as an efficient option to reduce
49 the urban heat island (UHI) effect that characterizes large contemporary urban concentrations,
50 thanks to the evapo-transpiration of the vegetal (lawn or trees) grown on them. Green roofs are
51 also interesting to reduce urban run-off. The substrates used in green roofs have to be light
52 enough and to present satisfactory water retention and transfer properties. Volcanic granular
53 substrates appear to be relevant in this context, and they are frequently used in green roofs, like
54 for instance in the case of the “Green Wave” of the Bienvenue building (Versini et al. 2017)
55 located close to Ecole des Ponts ParisTech in the Descartes campus of Marne la Vallée, 18 km
56 east of Paris (*Figure 1*). The green roof is covering three waves or 260 m length and 80 m wide,
57 on which a 20 cm thick layer of substrate has been placed. Actually, the use of substrates in urban
58 green roofs appears to be rather empirical to date, and very little data on their water retention and
59 transfer properties are available.

60 In this context, the paper describes the development and use of a specific controlled suction
61 device, based on both a tensiometry principle, through the hanging column technique, and the
62 axis translation method. The device is used to determine the water retention and transfer
63 properties of a volcanic substrate (VulkaTec Riebensahm GmbH 2016, Germany;
64 www.vulkatec.de) used in the Green Wave roof presented in *Figure 1*. Tensiometry controlled
65 suction was applied by means of the hanging column technique by connecting a tube to a ceramic
66 porous stone of 50 kPa air entry value on which a sample placed, and by imposing in the tube a
67 water level lower than that of the sample. The axis translation method was implemented by using
68 by applying air pressure on the top of the sample. The device was also used to determine the
69 hydraulic conductivity function during the transient phases resulting from step increases in
70 suction, by using the method proposed by Gardner (1956), accounting when necessary for the

71 impedance effects due to the permeability of the ceramic porous stone, by using Kunze and
72 Kirkham (1962)'s method.

73

74 2. Material and methods

75 2.1. Material

76 The VulkaTec volcanic material is presented in the photo of *Figure 2* and its main characteristics
77 are presented in *Table 1*. The material is very light with an average dry density of 1100 kg/m^3 so
78 as not to load the roof significantly. A percentage of 4 % of organic matter was determined by
79 using the French standard XPP94-047 1998, that consists in comparing the sample weight before
80 and after heating during at least 3 hours at temperature between 450 and 500 °C. The grain size
81 distribution curve of the substrate, determined by sieving following the French standard NFP94-
82 056 (1996) is presented in *Figure 3* (solid line). The distribution of fine particles ($< 80 \mu\text{m}$) was
83 obtained by sedimentation according to French standard NFP94-057 (1992). It can be noticed that
84 50% of the grains are larger than 1.6 mm with 10 % particles between 10 and 20 mm, in the
85 coarse range and 13 % fine particles smaller than $80 \mu\text{m}$. Also represented in *Figure 3* (dashed
86 curve) is the grain size distribution curve of the material used for the test, with all particles
87 smaller than 6 mm. Particles larger than 6 mm were discarded because we used a 70 mm diameter
88 cell. For the same volume, a specimen with large particles discarded will contain more small
89 particles, resulting in a larger porosity, in more water retained at a given suction, and in a larger
90 hydraulic conductivity. Given that the proportion of the coarse particles discarded is 20%, a
91 rough estimation of the over-estimation could be between 10 and 20 %. In *Table 1* are also
92 presented the curvature coefficient C_c ($C_c = (D_{30})^2 / (D_{60} \times D_{10}) = 1.95$) and the uniformity

93 coefficient C_u ($C_u = D_{60}/D_{10} = 55$). According to ASTM D2487-00 (2000), the material can be
94 regarded as well graded.

95

96 **2.2. Methods of controlling suction**

97 The various methods of controlling suction in soils include the hanging column technique
98 (Buckingham 1907), the axis translation technique (Richards 1941, 1947), the osmotic technique
99 (Zur 1966) and the vapour equilibrium technique (Esteban 1990). A detailed description of these
100 techniques and of their adaptation in geotechnical testing can be found in Delage (2002),
101 Vanapalli et al. (2008), Blatz et al. (2008), Delage and Cui (2008) and Fredlund et al. (2012).

102

103 Given that the volcanic substrate investigated here is granular with rather large grain sizes (see
104 *Figure 2*), it was initially decided to use the hanging column technique, because of its simplicity
105 to use and of its good accuracy in both the control of low suctions and the measurement of water
106 exchanges. However, one realized during the preliminary tests that, at the largest height imposed
107 in the hanging column technique (3.2 m, corresponding to a suction of 32 kPa), a significant
108 amount of water still remained in the substrate. It was then decided to impose larger suctions by
109 using the axis translation technique.

110 In both cases, tests were conducted on a 24 mm high specimen placed into a metal 70 mm
111 diameter cylindrical cell, in contact at its bottom with a 50 kPa air entry value ceramic porous
112 disk. A thin metal disk (2 mm thick) was placed on top of the sample, so as to monitor changes in
113 height by means of a displacement sensor (Mitutoyo Brand).

114

115 *The Hanging column technique*

116 The implementation of the hanging column technique is presented in *Figure 4*. The cell is
117 connected at its base through valve V2 to an outlet controlled by valve V3 and to a water
118 reservoir through valve V1. The cell is also connected through a central tube to a mobile device
119 that allows the imposition of water levels lower than that of the sample, so as to apply suction
120 defined by the difference in water level between the sample and the mobile part (up to 32 kPa at
121 the maximum height of 3.2 m).

122
123 The mobile device contains a smaller inner glass tube of $d_{\text{inn}} = 0.5 \text{ cm}$ and larger outer glass tube
124 of diameter $d_{\text{out}} = 1.5 \text{ cm}$. The inner tube is connected to the sample while the differential
125 pressure transducer is connecting the outer tube with the reference glass tube (*Figure 5*). This
126 pressure transducer (0.1 mm accuracy in water height) is able to provide high frequency
127 measurements that are necessary for the determination of the hydraulic conductivity function. A
128 monitoring rate of 10 s was adopted, chosen small enough to capture the change in the capillary
129 potential at small times through the change of the water level in the mobile device. This change is
130 detected as the height difference between the water levels either in the inner (valve V4 opened) or
131 the outer tube (valve V5 opened), and the water level in the reference tube used to indicate
132 constant reference water level. Most tubes used in the set-up are semi-rigid tubes made up of
133 polyamide, except that used in the mobile device (inner and outer tubes) and the reference tube
134 that are made up of glass.

135
136 The determination of the WRC along the drying path was carried out as follows:
137 Saturating the whole system: before starting, all the system has to be saturated, particularly the
138 tubes connected to the differential pressure transducer, because air bubbles in the tubes can result
139 in misleading data. Saturation was done by placing the reservoir filled with demineralized de-

140 aird water above the sample (*Figure 4*) and by opening valves V1 and V2 to let water infiltrate
141 the sample from the bottom to the top. Saturation was considered satisfactory when a thin layer of
142 water was observed on the sample top. Note that, whereas this procedure was satisfactory to
143 saturate the large inter-grains pores, the full saturation of the small pores existing within the fine
144 fraction ($13\% < 80 \mu m$) was less guaranteed. To improve saturation, the water circulation
145 between the bottom and the top of the specimen was let during one night. Then, valves V1 and
146 V2 were closed. Prior to running the test, the mobile device was placed in such a position that the
147 top of the inner tube full of water was at the same level as the top of the sample, resulting in
148 $h_k = 0$ (*Figure 4*). In order to check whether equilibrium was ensured, valve V2 (*Figure 4*) was
149 opened. If there was no water movement in the inner tube, the experiment could start. Otherwise,
150 the saturation procedure was repeated.

151 Imposing suction: two methods were used, according to the value of suction imposed.

152 i) At smaller suctions, starting from saturation, it was observed that suction increases mobilized a
153 significant volume of extracted water. Suction was then imposed by closing valves V2 and V5,
154 by filling the inner tube up to the top and by moving down the mobile device at a position
155 corresponding to the required suction. The water levels in the reference and outer tubes were
156 carefully adjusted at the starting level in both tubes (*Figure 5a*). The imposed suction was
157 defined by the difference in height between the top of the sample and the water level at the top of
158 the inner tube (h_k in *Figure 4*). Valves V2 and V5 were then opened, resulting in water being
159 extracted from the sample under the effect of increased suction. The extracted volume of water
160 (ΔV in *Figure 4*) flows from the top of the inner tube into the outer tube. It is monitored by the
161 differential pressure transducer that measures the height difference between the water levels in
162 the outer and reference tubes (ΔH_1 - *Figure 5a*). Once equilibrium is reached (after approximately

163 10 – 12 hours), a point on the WRC is obtained from the pair of values $(\theta_i, h_{k,i})$ from the
164 following equation:

$$165 \quad \theta_i = \theta_{i-1} - \Delta V_i / V_{\text{sample},(i-\frac{1}{2})} \quad (1)$$

166 where ΔV_i is the volume of water [L³] extracted from the sample, $V_{\text{sample},(i-\frac{1}{2})}$ the average sample
167 volume [L³] between the end and the start of the test, determined from the monitored changes in
168 height of the sample and $\theta_i - \theta_{i-1}$ the difference in volumetric water content [-] between the end
169 and the start of the test. Note however that the monitoring of the changes in sample height during
170 the tests indicated very small changes smaller than 0.5 mm (2%) along the whole test made up of
171 13 step increases in suction. The changes in height during each step were hence neglected.

172 ii) At larger suctions, the quantity of extracted water appeared to be much smaller and the
173 procedure was changed to improve accuracy. The initial water level in the inner tube was no
174 longer imposed at its top, but adjusted (by means of valve V3) at a lower level, in such a way that
175 overflow was avoided during water extraction from the sample. The changes in height in the
176 inner tube were then directly measured by the differential pressure transducer by closing valve
177 V5 and opening valve V4. The imposed suction was calculated at the end of the measurement
178 from the difference in height between the final water level in the inner tube and the top of the
179 sample (ΔH_2 - Figure 5b).

180 Before each new suction step, water levels in the outer (i) / inner (ii) and reference tubes were
181 adjusted to the same level by opening the bypass valve (Figure 5), in order to reset the
182 differential pressure transducer. Water levels in the outer (i) / inner (ii) and reference tubes were
183 then set to the required initial levels by carefully using valve V3, in order to eliminate extra water
184 through the outlet.

185

186 In this study, only the drying path was considered. But the apparatus can also be used along
187 wetting paths, along the following steps:

188 W1. Setting the initial position: the initial position of the mobile part is at the lowest vertical
189 level, i.e. the final position at highest suction reached during the drying path. The sample is hence
190 capable to store more water, thus a higher change in water level is expected. The water level
191 change is recorded in the outer tube while the inner tube is filled up with water to the top, and no
192 longer used during the test. Initial water levels in the outer and reference tubes should be set at
193 the top of the inner tube by opening valves V1, V4 and bypass and letting water flow over the top
194 of the inner tube. After reaching the required position, all valves and bypass should be closed.

195 W2. Imposing suction: by opening valves V5 and V2, water from the outer tube enters the
196 sample. The resulting decrease in water level in the outer tube is captured by the differential
197 pressure transducer.

198 W3. Reaching equilibrium: once equilibrium is reached, suction is calculated as the height
199 difference between the water level in the outer tube and the top of the sample. The corresponding
200 water content is calculated like during the drying path, but with an opposite sign because water
201 content is now increasing after each measurement ($\theta_i = \theta_{i-1} + \Delta V_i / V_{\text{sample},(i-\frac{1}{2})}$).

202 W4. Decreasing suction: to impose a lower suction, the mobile device is elevated, the outer
203 and reference tubes are filled again, as described in step W1, and the W2 procedure is repeated.

204 When a smaller change in water level in the outer tube is expected (lower suctions, higher water
205 content), the inner tube should be used, by closing valve V5 and using valve V4, unlike in step

206 W2.

207 W5. Final state of the wetting path: in order to saturate the sample, the mobile device should
208 be located at the initial position of the drying path with the water levels in the inner and reference

209 tubes corresponding to the sample top. In case of a difference in height between the level in the
210 inner tube and the top of the sample (if h_k marked in *Figure 4* is higher than zero) after reaching
211 equilibrium, the tubes should be refilled with water by opening valves V1, V4 and the bypass.
212 After closing valve V1 and the bypass and opening valve V2, without changing the vertical
213 position of mobile device, no water movement in the inner tube should occur. If this is not the
214 case, it means that the sample is not fully saturated and the refilling procedure should be
215 repeated.

216 As commented above, the hanging column technique was used for heights up to 3.2 *m*
217 corresponding to a maximum suction of 32 *kPa*. For higher suctions, the axis translation
218 technique was applied.

219

220 *The axis translation technique*

221 The axis translation technique was carried out by applying increasing air pressure on the top
222 sample surface. To do so, a cap connected to the air pressure supply source was placed on the top
223 of the cell, as indicated in *Figure 6*. Tests were carried out while keeping the sample and the
224 mobile device at the same level, above the differential manometer in order to monitor the changes
225 in height difference. The imposed suction was calculated as the difference between the air
226 pressure applied on the sample's upper surface and the change of water level inside the inner
227 tube.

228 Before each test, the water level in the inner tube should be put at the same level as the top of the
229 sample, and some space should be left above the water level to allow for some level increase with
230 no overflow during the measurement. Once the air pressure is imposed, valves V2 and V6 are
231 simultaneously opened, resulting in an increase of the water level in the inner tube, until
232 stabilization at equilibrium. The final suction is calculated as the difference between the applied

233 air pressure and the pressure corresponding to the water level increment in the inner tube,
234 captured by the pressure transducer. The corresponding water content is calculated by using
235 Equation (1). This methodology was applied for suctions up to 50 *kPa*, the air entry value of the
236 ceramic disk used. Higher suctions could be obtained with higher pressure and a ceramic disk of
237 higher air entry value.

238

239 **2.3. Determination of the hydraulic conductivity function**

240 *Saturated state*

241 The investigation on the hydraulic conductivity function (HCF) of the material started with the
242 determination of the saturated one. To do so, the cell containing the sample was disconnected
243 from the device and connected to a Mariotte's bottle filled with demineralized, de-aired water, so
244 as to run a constant head permeability test. Once the sample was saturated, the position of the
245 bottom of the thin tube that goes through the Mariotte's bottle was set in such a way that the
246 difference in height between the bottom of the thin tube and the top surface of the sample
247 represented the imposed water head ΔH [L]. The water level in the Mariotte's bottle had always
248 to be above the bottom of the thin tube, in order to ensure a constant imposed water head. By
249 measuring the water level change in the Mariotte's bottle ΔH [L] and the time necessary for
250 obtaining this change Δt [T], the flux q [L/T] can be calculated.

$$251 \quad q_n = \frac{\Delta H_n A_{mariotte}}{\Delta t_n A} \quad n = 1, 2, 3 \quad (2)$$

252 where $A_{Mariotte}$ is the cross-section area of the Mariotte's bottle, decreased by the area of the thin
253 tube. The saturated hydraulic conductivity K_s is then calculated using Darcy's law.

$$254 \quad K_{s,n} = \frac{q_n}{\Delta H_n} H_{sample} \quad n = 1, 2, 3 \quad (3)$$

255 The procedure was repeated for three different imposed water heads ($n = 1, 2, 3$), that were
256 adjusted by changing the altitude of the bottom of the thin tube.

257

258 *Unsaturated states*

259 The various existing methods of measuring the hydraulic conductivity functions in unsaturated
260 have been described in various papers or textbooks including Masrouri et al. (2008) and Fredlund
261 et al. (2012). In steady state methods (Corey 1957, Klute 1972, Olsen et al. 1985, among others),
262 a constant flow is imposed in a specimen put under given values of controlled suction. These
263 methods are known to be rather long and tedious, due in particular to the need of very precisely
264 measuring tiny transient flows along rather long periods of time. Alternatively, transient methods,
265 in which the water outflow from the specimen submitted to suction steps is monitored (Gardner
266 1956, Miller and Elrick 1958, Kunze and Kirkham 1962), are known to be easier to perform, with
267 simpler equipment (Masrouri et al. 2008). For these reasons, transient methods were used in this
268 work.

269 The HCF was hence determined by applying suction steps and monitoring the resulting changes
270 in water content $V(t)$ with time until equilibration, by means of the differential pressure
271 transducer. It was planned to calculate the hydraulic conductivity of the specimen by using
272 Gardner's method (Gardner 1956). This method assumes that the change in suction for each step
273 is small, in such a way that the diffusion coefficient $D(h_k)$ can reasonably be considered constant
274 during the test:

$$275 \quad D(h_k) = D = \frac{K(h_k)}{C(h_k)} = \frac{K(h_k)\Delta h_k}{\Delta\theta} \quad (4)$$

276 where $C(h_k)$ is the average slope of the WRC [L^{-1}] along the suction step corresponding to Δh_k
277 [L] and $K(h_k)$ is the hydraulic conductivity [L/T]. Based on the analytical solution of the diffusion

278 equation expressed in terms of a Fourier series, Gardner proposed an estimation of the water
 279 conductivity using the monitored volume $V(t)$ [L³] of water extracted from the sample:

$$280 \quad V(t) = V_{\infty} \left(1 - \frac{8}{\pi^2} \sum_{n=1,3,5,\dots}^{\infty} \frac{1}{n^2} e^{-\left(\frac{n}{2}\right)^2 \pi^2 \frac{t}{T}} \right) \quad (5)$$

$$281 \quad T = \frac{H_{sample}^2 C(h_k)}{K(h_k)} = \frac{H_{sample}^2}{D} \quad (6)$$

282 where V_{∞} is the total amount of water extracted during the suction step [L³]. As commented
 283 above, we observed in this work that the sample height H_{sample} remained reasonably constant, we
 284 hence adopted $H_{sample} = 2.4 \text{ cm}$.

285 Gardner's method is based on the fact that only the first member ($n = 1$) of the Fourier series in
 286 Equation (5) can be taken into account as a reasonable approximate solution, acceptable after $t >$

287 $t_{bound} = \frac{4H_{sample}^2}{3\pi^2 D}$. In such conditions, the equation corresponding to the first member of

288 Equation (5) can be written as:

$$289 \quad \ln[V_{\infty} - V(t)] = \ln \frac{8V_{\infty}}{\pi^2} - \pi^2 \frac{Dt}{4H_{sample}^2} \quad (7)$$

290 showing that the term $\ln[V_{\infty} - V(t)]$ becomes a linear function of time t , with a slope depending
 291 on the diffusion coefficient D .

292 The hydraulic conductivity $K(h_k)$ can then be calculated using the following equation:

$$293 \quad K(h_k) = \frac{D\Delta\theta}{\Delta h_k} \quad (8)$$

294 The experimental data obtained in this work indicated that Gardner's method is more relevant at
 295 higher suctions, in which i) less water exchanges occurred, ii) the condition of constant suction is
 296 ensured and iii) the assumption about a constant diffusion coefficient D is more satisfactorily
 297 fulfilled.

298 However, Gardner's method cannot be directly used when the saturated hydraulic conductivity of
299 the ceramic disk is smaller than that of the sample. Experimental data showed that this occurred
300 during the first steps at low suction from the saturated state, during which higher hydraulic
301 conductivity values are obtained. To cope with the cases in which impedance effects due to the
302 ceramic disk occur, the method proposed by Kunze and Kirkham (1962) was adopted.

303

304 *Kunze and Kirkham's method*

305 Kunze and Kirkham (1962) considered the solution of the consolidation equation applied for
306 various layers of soil with different hydraulic conductivities. Their solution is graphically
307 presented through various curves showing the changes in $V(t)/V_\infty$ with respect to the variable
308 $\lambda_1^2 Dt / H_{sample}^2$ (see *Figure 11*), in which the parameter λ_1 is the first solution of equation
309 $a\lambda_n = \cot\lambda_n$ and a is the ratio between the impedance of the ceramic disk and that of the sample.
310 The various curves in *Figure 11* correspond to various values of parameter a .

311 In order to determine the hydraulic conductivity $K(h_k)$ of the sample, it is required to estimate
312 parameters a and λ_1 , by fitting the experimental data (presented in the form $V(t) / V_\infty$ versus t)
313 with one of the theoretical curves. Kunze and Kirkham (1962) remarked that only a portion of the
314 experimental data corresponded to the theoretical curves, so they recommended to rather fit the
315 curves at small times, for which more accurate values of λ_1^2 are obtained. The choice of the
316 adequate theoretical curve provides the value of parameter a . It is then possible to determine the
317 corresponding parameter λ_1 from the table presented in the paper of Kunze and Kirkham (1962).
318 It is also necessary to graphically determine the reference time t_{RP} that corresponds to
319 $\lambda_1^2 Dt / H_{soil}^2 = 1$ (vertical arrow in *Figure 11*). Finally, the diffusion coefficient is calculated as
320 $D = H_{soil}^2 / \lambda_1^2 t_{RP}$ and the hydraulic conductivity as $K = D\Delta\theta / \Delta h_0$.

321

322 Another way to explore a possible impedance effect due to the ceramic porous disk is to apply
323 Darcy's law to the flux going through the saturated ceramic disk, as follows:

$$324 \quad h_{k,top} = h_k + \Delta z_s \frac{\Delta V}{\Delta t} \frac{1}{A_{cs} K_{cs}} \quad (9)$$

325 where $h_{k,top}$ is the suction [L] at the top of the ceramic disk, Δz_s its thickness [L], A_{cs} its cross
326 section area [L²] (7 cm diameter), and ΔV is the volume [L³] extracted from the sample during the
327 time interval Δt [T].

328 The change in suction at the top of the ceramic disk can hence be derived from the monitoring of
329 the extracted water volume ΔV with respect to time. In the lack of any impedance effect, both
330 suction values at top and bottom should be equal.

331

332 3. Experimental results

333 3.1. Water retention curve

334 *Figure 7* shows the continuous monitoring of the changes in suction with both the hanging
335 column technique (steps 1 to 10) and the axis translation technique (steps 11 to 13). The outer
336 tube was used for steps 1 and 2 that mobilized larger water volumes (valve V4 closed, valve V5
337 opened, see *Figure 5a*), while the subsequent 11 steps (3 – 13) were made by using the inner tube
338 (valve V4 opened, valve V5 closed, see *Figure 5b*). In the former case, the imposed suction
339 remains constant (*Figure 8a*, solid line with squares – the dashed line with triangles will be
340 commented later on), while in the latter case (3 - 13), the initial instantaneous drop in height Δh_o
341 (increase in suction) is followed by a slight progressive increase in height, corresponding to a
342 slight decrease in suction (see for example steps 11 - 12 in *Figure 8b*).

343 The corresponding drying path of the WRC is presented in *Figure 9*, in which the changes in
 344 volumetric water content θ are plotted with respect to changes in suction. The curve evidences a
 345 significant decrease in water content for the initial steps at low suctions, with θ decreasing from
 346 the initial value of 0.45 down to 0.29 upon application of the first suction step of 2.1 *kPa*. The
 347 increment in volumetric water content progressively decreases afterwards, with a decrease in θ to
 348 0.25 at a suction of 4.2 *kPa*. The curve finally becomes almost linear at suction larger than
 349 14.2 *kPa*, indicating that the further suction increments extract small quantities of water. A final
 350 value of 0.16 is reached at 49.6 *kPa*. Good compatibility is observed between the section
 351 obtained with the hanging column technique (1 – 10) and that with the axis translation method
 352 (11 – 13).

353 *Figure 9* also shows that a good fitting is obtained by using the WRC expressions of Brooks and
 354 Corey (1964) and van Genuchten (1980), as follows:

355 - van Genuchten (vG): $\theta = \theta_r + \frac{\theta_s - \theta_r}{[1 + (\alpha h_k)^n]^m}$; with $m = 1 - \frac{1}{n}$ (10)

356 where θ_s is the saturated volumetric water content ($\theta_s = 0.45$, see *Figure 9*), θ_r [-] the residual one,
 357 $\alpha = 1 / h_a$ [L^{-1}] where h_a [L] is the air entry value expressed in water height, and n [-] an
 358 empirical parameter;

359 - Brooks & Corey (BC): $\theta = \theta_r + (\theta_s - \theta_r) \left(\frac{h_k}{h_a}\right)^{-\lambda}$ (11)

360 where λ [-] is an empirical parameter.

361 The fitting of the parameters of both vG and BC curves were made by first adopting values of h_a
 362 and θ_r , taken equal to 3.2 cm and 0.11, respectively. The best fitting was obtained with $n = 1.35$
 363 (vG expression) and $\lambda = 0.35$ (BC expression).

364

365 **3.2. Hydraulic conductivity function**

366 *Saturated state*

367 *Figure 10* shows the data obtained from the steady-state permeability test, expressed in terms of
368 changes in fluxes q_n with respect to the hydraulic gradient ($i = \Delta\Pi_n / H_{sample}$, see Equation 3). The
369 slope of the linear regression corresponding to the three measured points ($n = 1, 2, 3$) and to point
370 $(0, 0)$ provides a value $K_s = 8.11 \times 10^{-6} \text{ m/s}$.

371
372 The same approach carried out on the ceramic porous stone provided a value $K_{cs} = 4.02 \times 10^{-8}$
373 m/s , confirming that the hydraulic conductivity of the saturated ceramic porous stone is
374 significantly smaller than that of the saturated material. As a consequence, Kunze and Kirkham's
375 method was used to interpret the data of the first suction steps (1 and 2) applied from the
376 saturated state.

377
378 *Unsaturated states*

379 *Figure 11* presents the experimental data of steps 1 and 2 presented in terms of changes in
380 $V(t)/V_\infty$ with respect to a log scale of $\lambda_1^2 D t_{RP} / H_{sample}$, as proposed by Kunze and Kirkham. For
381 step 1, *Figure 11* shows excellent agreement of the data with the theoretical curve of parameter
382 $a = 1$. The corresponding value of parameter λ_1^2 is 0.74, according to Kunze and Kirkham
383 (1962)'s graph, while the reference time t_{RP} is 47 min (2800 s). Finally, a hydraulic conductivity
384 $K(s) = 2.14 \times 10^{-7} \text{ m/s}$ is obtained for a suction of 2.1 kPa. This value is larger than that of the
385 ceramic disk ($K_{cs} = 4.02 \times 10^{-8} \text{ m/s}$), confirming the necessity of accounting for the impedance
386 effect of the porous stone.

387 Similarly, a value $a = 0.142$ is obtained for step 2, with $\lambda_1^2 = 1.90$ with $t_{RP} = 24 \text{ min}$ (1440 s),
388 resulting in a hydraulic conductivity value of $3.64 \times 10^{-8} \text{ m/s}$, slightly smaller than that of the
389 ceramic porous stone.

390 The calculations of the changes with time of the suction imposed on the top of the ceramic disk
391 according to Equation 10 are presented in *Figure 8a* for step 1 and 2 (dashed line with triangles).
392 As expected, they confirm the perturbation due to the low permeability of the ceramic disk. This
393 perturbation is stronger during step 1, in which almost 3 hours are necessary to reach the desired
394 2.1 kPa suction at the top, compared to step 2 in which the 4.2 kPa imposed suction is reached at
395 the top after less than 2 hours.

396
397 Prior to use Gardner's method, the assumption of constant suction during each suction step has to
398 be checked. Inspection of the suction steps applied for suctions higher than 4.1 kPa (steps 3 – 13,
399 *Figure 7*) showed that the water level in the inner tube was slightly rising at the start of the step,
400 hence decreasing the suction. The level changes in the inner tube during steps 3 and 4 are around
401 7.5 % of the imposed suction and 30 % of the imposed suction increment. These two steps do not
402 reasonably ensure the constant suction condition, they will not be considered for the
403 determination of the HCF. For suctions higher than 10 kPa (measurements 5 – 13, *Figure 7*), the
404 level increase in the tube is smaller (less than 4 % of the imposed suction and less than 12 % of
405 the imposed suction increment), and suction changes are considered to be reasonably compatible
406 with the use of Gardner's method (see for example steps 11 and 12 in *Figure 8b*).

407
408 The application of Gardner's method is presented in *Figure 12*, that shows the changes in
409 $\ln[V_\infty - V(t)]$ with respect to time for the measurements made during steps 2 and 5 – 13 (see
410 Equation 7). In all cases, the linearity of the $\ln[V_\infty - V(t)]$ function is satisfactory. As

411 recommended by Gardner, the fitting is only based on the points corresponding to $t > t_{bound}$. The
412 values of t_{bound} , calculated for each stage, are given in the graph of each step. Values are included
413 between 0.2 and 2 h, depending of the value of D . Note that step 2 was also considered here, so
414 as to compare the data with that of Kunze and Kirkham's method, that is more appropriate, given
415 possible impedance effects.

416
417 *Figure 13* shows the hydraulic conductivities obtained using the three different methods: i)
418 saturated hydraulic conductivity, using the constant-head permeability test, ii) unsaturated
419 hydraulic conductivity at lower suctions, using Kunze and Kirkham's method (steps 1 and 2) and
420 iii) unsaturated hydraulic conductivity at larger suctions, using Gardner's method (steps 2' and 5
421 to 13).

422
423 One observes that the hydraulic conductivity at step 2' provided by Gardner's method is
424 somewhat smaller than that (step 2) given by Kunze and Kirkham's method. This is compatible
425 with the impedance effect due to the low permeability of the ceramic disk, that indicates that
426 Gardner's method is not fully satisfactory for step 2. Note however that the difference in
427 hydraulic conductivity is not that large (3.64×10^{-8} m/s for Kunze and Kirkham and 1.64×10^{-8}
428 m/s for Gardner's method).

429
430 All the points obtained by the three methods are in reasonable agreement and provide the
431 decrease in hydraulic conductivity with increased suction along the drying path. In the first 5
432 steps, a large decrease of 4 orders of magnitude is observed from 10^{-5} m/s (saturated state) down
433 to 10^{-9} m/s at a suction of 10.4 kPa, and the hydraulic conductivity then stays between 10^{-9} and
434 10^{-10} m/s for steps 5 to 13, corresponding to suctions between 10.4 and 49.6 kPa.

435 The results are also compared with the curves obtained by using the mathematical expressions of
 436 the relative hydraulic conductivity ($K_r(h_k) = K(h_k) / K_s$) derived from the WRC formulations of
 437 Brooks and Corey (1964) and van Genuchten (1980) according to Mualem (1970)'s approach
 438 (Equations 10 and 11), as follows:

439 - van Genuchten:
$$K_r(h_k) = \frac{\{1 - (\alpha h_k)^{n-1} [1 + (\alpha h_k)^n]^{-m}\}^2}{[1 + (\alpha h_k)^n]^{m/2}} \quad (12)$$

440 - Brooks & Corey:
$$K_r(h_k) = \left(\frac{h_k}{h_a}\right)^{-2-5\lambda/2} \quad (13)$$

441 The curves obtained with the parameters obtained from the WRC curves, also represented in
 442 *Figure 13*, do not satisfactorily fit with the experimental data. Both formulations underestimate
 443 the hydraulic conductivity, with a better correspondence observed with the Brooks and Corey
 444 formulation. Because of this poor correspondence, it was decided to propose a power law, fitted
 445 by using the root-mean-square-deviation (RMSD) method. This solution can be written in the
 446 following form:

447
$$K(s) = a_1 \times s^{b_1} \quad (14)$$

448 with $a_1 = 5.38 \times 10^{-7}$ and $b_1 = -2.283$, giving:

449
$$K(s) = 5.38 \times 10^{-7} \times s^{-2.283} \quad (15)$$

450 The corresponding expression of the relative permeability is then:

451
$$\frac{K(s)}{K_s} = a_2 s^{b_1} = 6.63 \times 10^{-2} \times s^{-2.283} \quad (16)$$

452 In order to present the right side of Equation (16) in the relative form as well, coefficient a_2 can
 453 be written as follows:

454
$$a_2 = \left(\frac{1}{s_0}\right)^{b_1} \rightarrow s_0 = a_2^{-\frac{1}{b_1}} = 0.305 \quad (17)$$

455 where s_0 is the suction value corresponding to the air entry value, expressed in $[kPa]$. The final
456 form of the equation reads:

$$457 \frac{K(s)}{K_s} = \left(\frac{s}{s_0}\right)^b \quad (18)$$

458 with $s_0 = 0.305 \text{ kPa}$ and $b = b_1 = -2.283$.

459

460 **4. Conclusion**

461 The new device developed in this work allowed to determine the water retention curve and the
462 hydraulic conductivity function of a light coarse material used as substrate in an urban green roof.

463 In a first estimation, it was estimated than the hanging column technique of controlling suction,
464 with a maximum height of 3.2 m (suction 32 kPa) would have been satisfactory, but it was finally
465 necessary to impose larger suctions by using the axis translation technique. This adaptation was
466 rather simple to carry out, finally allowing to run the whole test by using both techniques on the
467 same specimen in the same cell between the saturated state and a maximum suction of 49.6 kPa ,
468 with a good comparability between the experimental data obtained by the two techniques.

469 The advantage of the hanging column technique is to allow for a very good precision in the
470 control of both the suction and the water exchanges, made possible by using a differential
471 pressure sensor with an accuracy of 0.1 mm in height. A specific system based on the use of both
472 an inner and an outer tube was also developed so as to improve the accuracy of the measurements
473 along the range of the applied suctions. This good accuracy was necessary, given the significant
474 changes in volumetric water content observed during the first application of a suction as low as
475 2.1 kPa , that resulted in a significant decrease from 0.45 to 0.29 .

476

477 Starting from a saturated state, the WRC exhibited a drastic decrease under a small suction of
478 2.1 *kPa*, in link with the coarse nature of the granular substrate, followed by a progressive
479 decrease down to a water content of 0.16 at 49.6 *kPa*. Both the van Genuchten and Brooks and
480 Corey mathematical expressions fitted quite nicely with the experimental data.

481
482 The good accuracy in the measurements of suction and water exchanges also allowed to
483 simultaneously determine, in a simple fashion, the hydraulic conductivity function from the
484 monitoring of the water exchanges resulting from the step changes in suction. At lower suctions
485 (2.1 and 4.2 *kPa*) and higher hydraulic conductivity, it was necessary to account for the
486 impedance effects due to the 50 *kPa* air entry value ceramic disk by successfully using Kunze
487 and Kirkham's method. Gardner's method was used at larger suctions, and a good comparability
488 was observed from the experimental data from each technique. Another advantage of the device
489 is to simply allow for the determination of both the water retention curve and the hydraulic
490 conductivity function of the coarse material. Unsurprisingly, the HCF function exhibit a trend
491 similar to that of the WRC, with a decrease of around 3 orders of magnitude between the
492 saturated state and that at a suction of 4.2 *kPa*, whereas all the data between 10.4 and 49.6 *kPa*
493 were comprised between 10^{-9} and 10^{-10} m/s.

494
495 The experimental HCF data were compared with the analytical expressions derived from the
496 WRC expressions of van Genuchten and Brooks and Corey, based on Mualem's approach. In
497 both cases, these expressions appeared to significantly underestimate the experimental HCF, with
498 however better results with Brooks and Corey's expression, that was less than one order of
499 magnitude below the experimental data. These expressions of the HCF are often used in the lack
500 of experimental data, and the difference observed in this work confirm the need of having

501 operational devices for the simultaneous experimental determination of the water retention curve
502 and the hydraulic conductivity function in granular materials such as the green roof substrate
503 investigated in this work.

504

505 **5. References**

506 ASTM D2487-00: Standard Practice for Classification of Soils for Engineering Purposes (Unified
507 Soil Classification System), *Annual Book of ASTM Standards*, ASTM International, West
508 Conshohocken, PA, 2000.

509 Blatz, J., Cui, Y.-J., Oldecop, L.A., 2008, "Vapour equilibrium and osmotic technique for suction
510 control," *Geotech. Geol. Eng.*, doi:10.1007/s10706-008-9196-1

511 Brooks, R.H, Corey, A. T., 1964, "Hydraulic properties of porous media," *Hydrology papers*,
512 No.3.

513 Corey, A.T., 1957, "Measurement of water and air permeability in unsaturated soil," *Soil Sci.*
514 *Soc. Am. Proc.*, Vol. 21, No. 1, pp. 7–10.

515 Buckingham, E., 1907, "Studies on the movement of soil moisture," Bull 38 USDA, Bureau of
516 Soils, Washington DC.

517 Cui, Y. J., Delage, P., Alzoghbi, P., 2003, "Retention and transport of a hydrocarbon in a silt,"
518 *Géotechnique*, Vol. 53, No. 1, pp. 83-91.

519 Delage, P., 2002, "Experimental unsaturated soil mechanics: State-of-art-report," 3rd International
520 conference on unsaturated soils, Vol. 3, Recife.

521 Delage, P., Cui, Y.-J., 2008, "An evaluation of the osmotic technique of controlling suction,"

522 *Geomech. Geoengin. Int. J.*, Vol. 3, No. 1, pp. 1–11.

523 Esteban, F., 1990, “Caracterización de la expansividad de una roca evaporítica. Identificación de
524 los mecanismos de hinchamiento”, Tesis doctoral de la Universidad de Cantabria, Santander.

525 Fredlund, D. G., Rahardjo, H. and Fredlund M. D., 2012, *Unsaturated Soil Mechanics in*
526 *Engineering practice*, Wiley, New York.

527 Fredlund, D. G., and Xing., A., 1994, "Equations for the soil-water characteristic curve," *Can.*
528 *Geotech. J.*, Vol. 31, pp. 521-532.

529 Gardner, W. R., 1956, "Calculation of Capillary Conductivity from Pressure Plate Outflow Data."
530 *Soil Science Society Proceeding*, Vol. 20, pp. 317 - 320.

531 Klute, A., 1972, “The determination of the hydraulic conductivity and diffusivity of unsaturated
532 soils,” *Soil Sci.*, Vol. 113, No. 4, pp. 264-276.

533 Kunze, R. J., and Kirkham, D., 1962, “Simplified Accounting for membrane impedance in
534 Capillary Conductivity Determinations,” *Soil Sci. Soc. Am. Proc.*, Vol. 26, pp. 421-426.

535 Li, Y., and Babcock Jr., R. W., 2016, “A Simplified Model for Modular Green Roof Hydrologic
536 Analysis and Design,” *Water*, Vol. 8, No. 343, pp. 1 – 13.

537 Masrouri, F., Bicalho, K.V., Kawai, K., 2008, “Hydraulic testing in unsaturated soils,” *Geotech.*
538 *Geol. Eng.*, Vol. 26, pp. 691 – 704, doi:10.1007/s10706-008-9202-7.

539 Miller, E., Elrick, D., 1958, “Dynamic determination of capillary conductivity extended for non-
540 negligible membrane impedance,” *Soil Sci. Soc. Am. Proc.*, Vol. 22, pp. 483–486.

541 Mualem, Y., 1976, “A New Model for Predicting the Hydraulic Conductivity of Unsaturated
542 Porous Media,” *Water Resources Research*, Vol. 12, No. 3, pp. 513-522.

543 NFP94-056, "Analyse granulométrique - Méthode par tamisage à sec après lavage," French
544 Standard, AFNOR Editions, Paris La Défense Cedex, 1996.

545 NFP94-057, "Analyse granulométrique des sols - Méthode par sédimentation," French Standard,
546 AFNOR Editions, Paris La Défense Cedex, 1992.

547 Olsen, H.W., Nichols, R.W., Rice, T.L., 1985, "Low gradient permeability methods in a triaxial
548 system," *Géotechnique*, Vol. 35, No. 2, pp. 145–157.

549 Richards, L.A., 1941, "A pressure-membrane extraction apparatus for soil solution," *Soil Sci.*,
550 Vol. 51, No. 5, pp. 377–386.

551 Richards, L.A., 1947, "Pressure-membrane apparatus – construction and use," *Agric. Eng.*, Vol.
552 28, pp. 451–460.

553 Vanapalli, S.K., Sharma, R.S., Nicotera, M.V., 2008, "Axis-translation and negative water
554 column techniques for suction control," *Geotech. Geol. Eng.*, Vol. 26, pp. 645 – 660,
555 doi:10.1007/s10706-008-9206-3.

556 van Genuchten, M. Th., 1980, "A Closed-form Equation for Predicting the Hydraulic
557 Conductivity of Unsaturated Soils," *Soil Sci. Soc. Am. J.*, Vol. 44, pp. 892-898.

558 Versini, P.A., Gires, A., Fitton, G., Tchiguirinskaia, I., Schertzer, D., 2017, "La Vague Verte de
559 l'ENPC: un site pilote de Blue Green Dream pour évaluer les variabilité spatio-temporelles du
560 bilan hydrologique d'une infrastructure végétale - ENPC Blue Green Wave: a Blue Green
561 Dream pilot site to assess spatio-temporal variability of hydrological components in green
562 infrastructures," *La Houille Blanche*, Accepted for publication.

563 VulkaTec Riebensahm GmbH, "Assurance qualité - Vulkaplus intensiv 0-12,"
564 GUTEGEMEINSCHAFT SUBSTRATE FUR PFLANZEN E.V., Kretz, Germany, 2016.

565 XPP94-047, "Détermination de la teneur pondérale en matières organiques d'un matériau,"

566 French Standard, AFNOR Editions, Paris La Défense Cedex, 1998.

567 Zur, B., 1966, "Osmotic control the matric soil water potential," *Soil Sci.*, Vol. 102, pp. 394–398

568

569 **Acknowledgements**

570 The authors are indebted to the VulkaTec Riebensahm GmbH Company (Germany) for providing

571 the substrate material investigated in this study. They are also grateful to the two anonymous

572 reviewers for their comments, that helped improving the quality of the paper.

573 *Table 1. Basic characteristics of “Green Wave” substrate*

Dry density	Porosity	Curvature coefficient	Uniformity coefficient	Percentage of organic matter
ρ_s [kg/m ³]	n [-]	C_c [-]	C_u [-]	C_{MOC} [%]
1100	0.448	1.95	55	4

574

575 **List of Figures**

576 *Figure 1. The “Green Wave” of the Bienvenue building located close to Ecole des Ponts*
 577 *ParisTech, Marne la Vallée*

578 *Figure 2. Photo of the volcanic substrate used for the “Green Wave”*

579 *Figure 3. Grain size distribution curve of the volcanic substrate*

580 *Figure 4. General lay-out of the hanging column system*

581 *Figure 5. Description of the two procedures used: a) change in water level observed the in outer*
 582 *tube (ΔH_1) with valve V4 closed and valve 5 opened; b) change in water level observed in*
 583 *the inner tube (ΔH_2) with valve 4 opened and valve 5 closed.*

584 *Figure 6. Application of the axis translation technique*

585 *Figure 7. Continuous monitoring of the imposed suctions during the 13 steps, provided by the*
 586 *differential pressure transducer.*

587 *Figure 8. Zoom of the suction changes (solid line with rectangles – imposed suction; dashed line*
 588 *with triangles – calculated suction at the top of the ceramic disk): a) steps 1 and 2; b) steps*
 589 *11 and 12*

590 *Figure 9. Water retention curve obtained using both techniques of controlling suction (hanging*
 591 *column and axis translation)*

592 *Figure 10. Data of the constant water head hydraulic conductivity measurement of the saturated*
 593 *material.*

594 *Figure 11. Kunze and Kirkham's method applied to measurements 1 and 2 (arrow indicates t_{RP})*

595 *Figure 12. Data from Gardner's method, suction steps 2 and 5 – 13*

596 *Figure 13. Hydraulic conductivity function (HCF)*

597



598

599 *Figure 1. The “Green Wave” of the Bienvenue building located close to Ecole des Ponts*
600 *ParisTech, Marne la Vallée*

601

602

603

604

605

606

607

608

609



610

611 *Figure 2. Photo of the volcanic substrate used for the “Green Wave”*

612

613

614

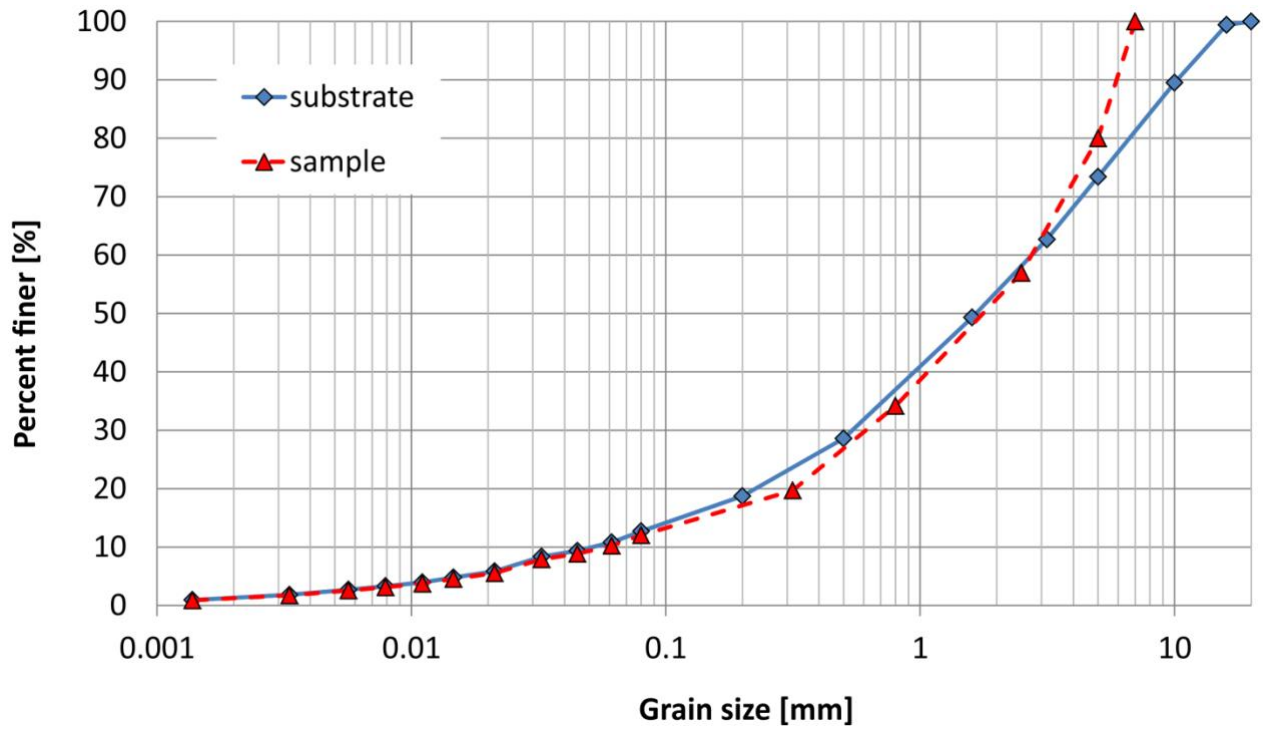
615

616

617

618

619



620

621 *Figure 3. Grain size distribution curve of the volcanic substrate*

622

623

624

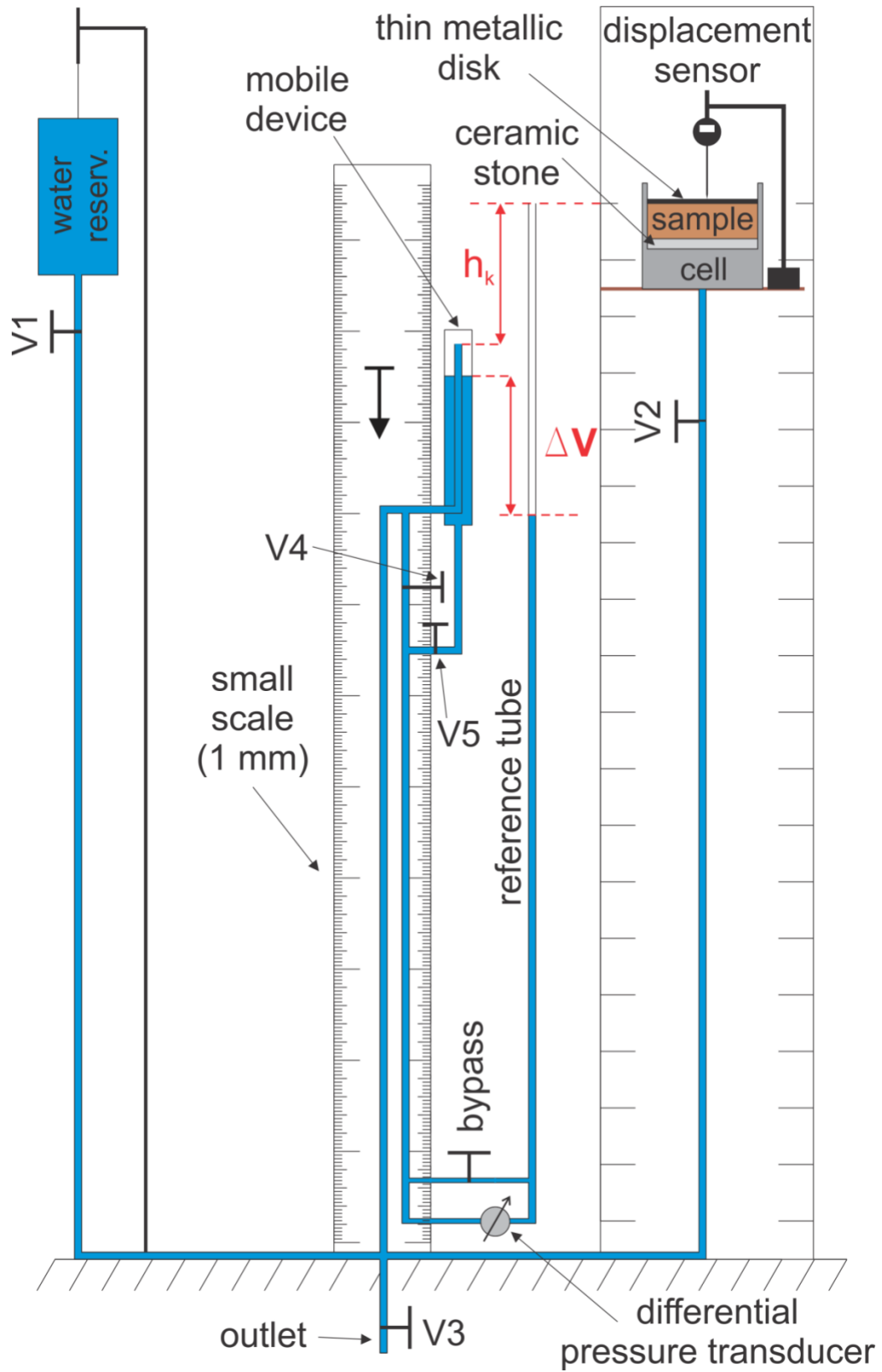
625

626

627

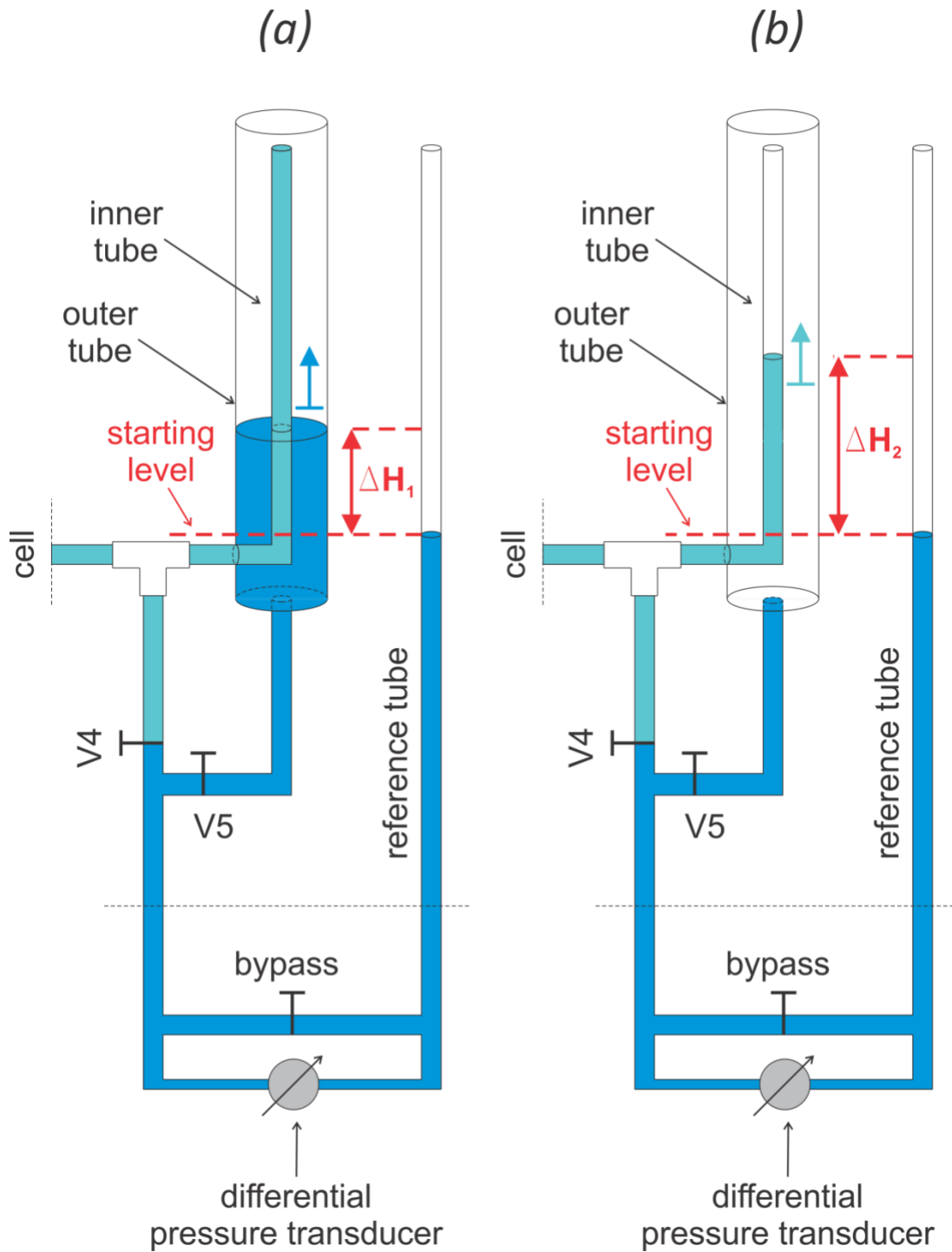
628

629



630

631 *Figure 4. General lay-out of the hanging column system*

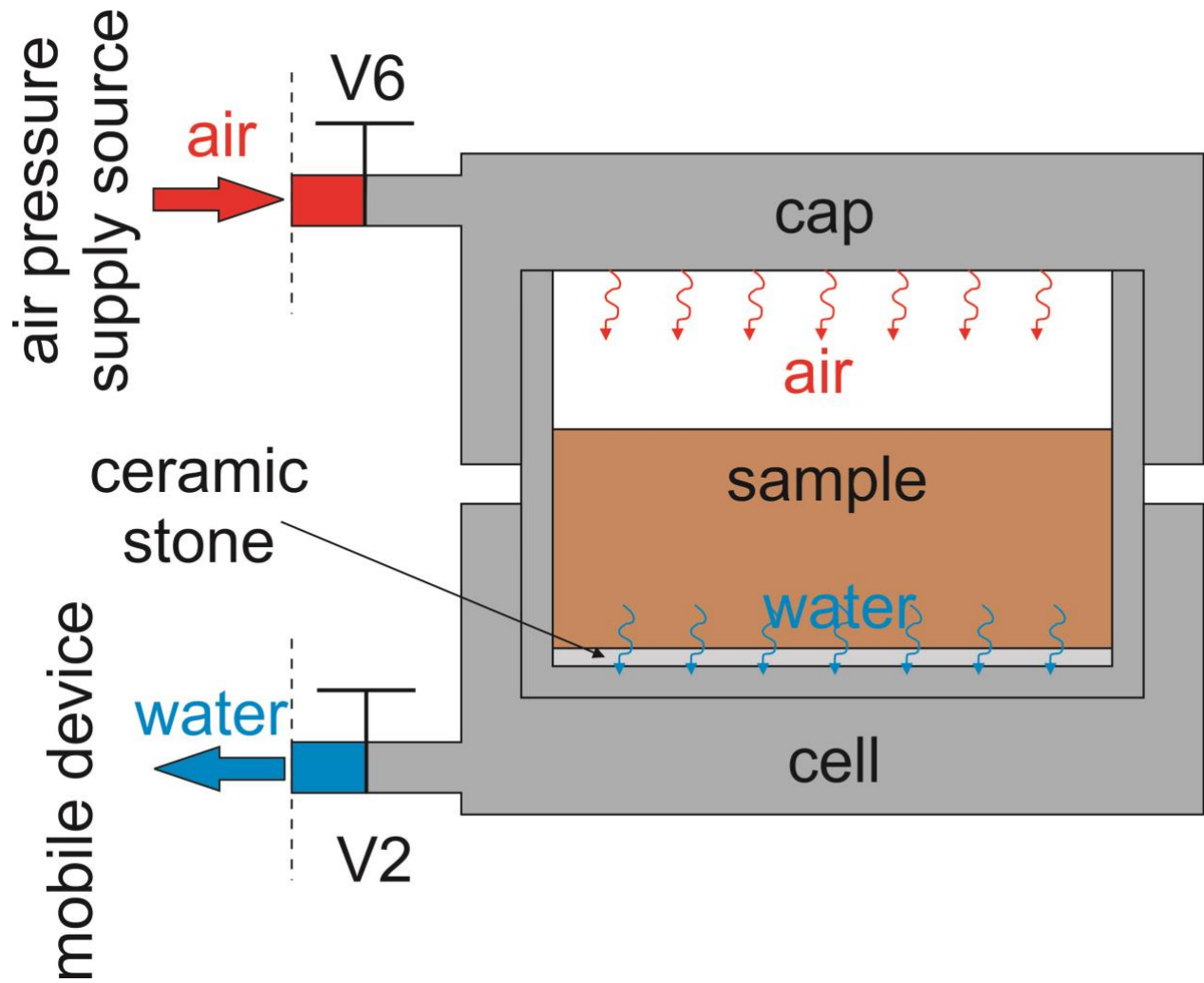


632

633 *Figure 5. Description of the two procedures used: a) change in water level observed the in outer*

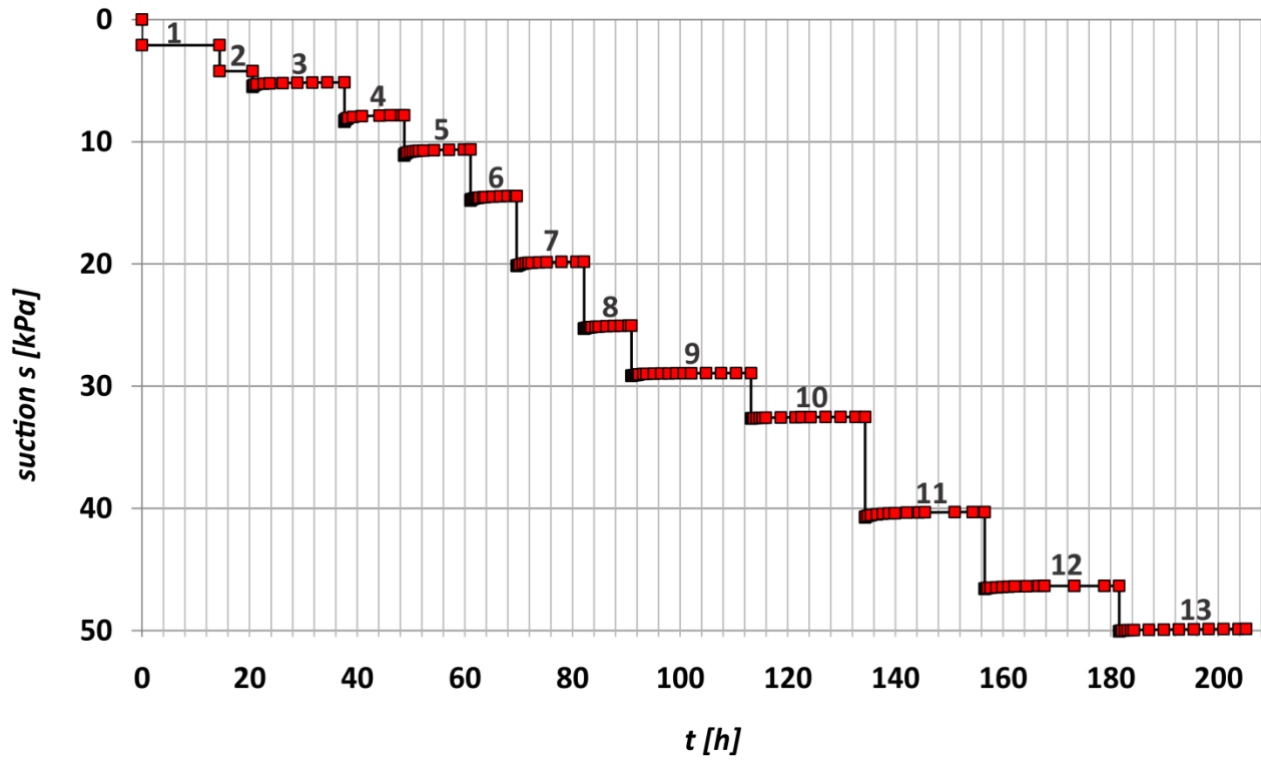
634 *tube (ΔH_1) with valve V4 closed and valve 5 opened; b) change in water level observed in the*

635 *inner tube (ΔH_2) with valve 4 opened and valve 5 closed.*



636
 637
 638
 639
 640
 641
 642
 643
 644
 645

Figure 6. Application of the axis translation technique



646

647 *Figure 7. Continuous monitoring of the imposed suctions during the 13 steps, provided by the*
 648 *differential pressure transducer.*

649

650

651

652

653

654

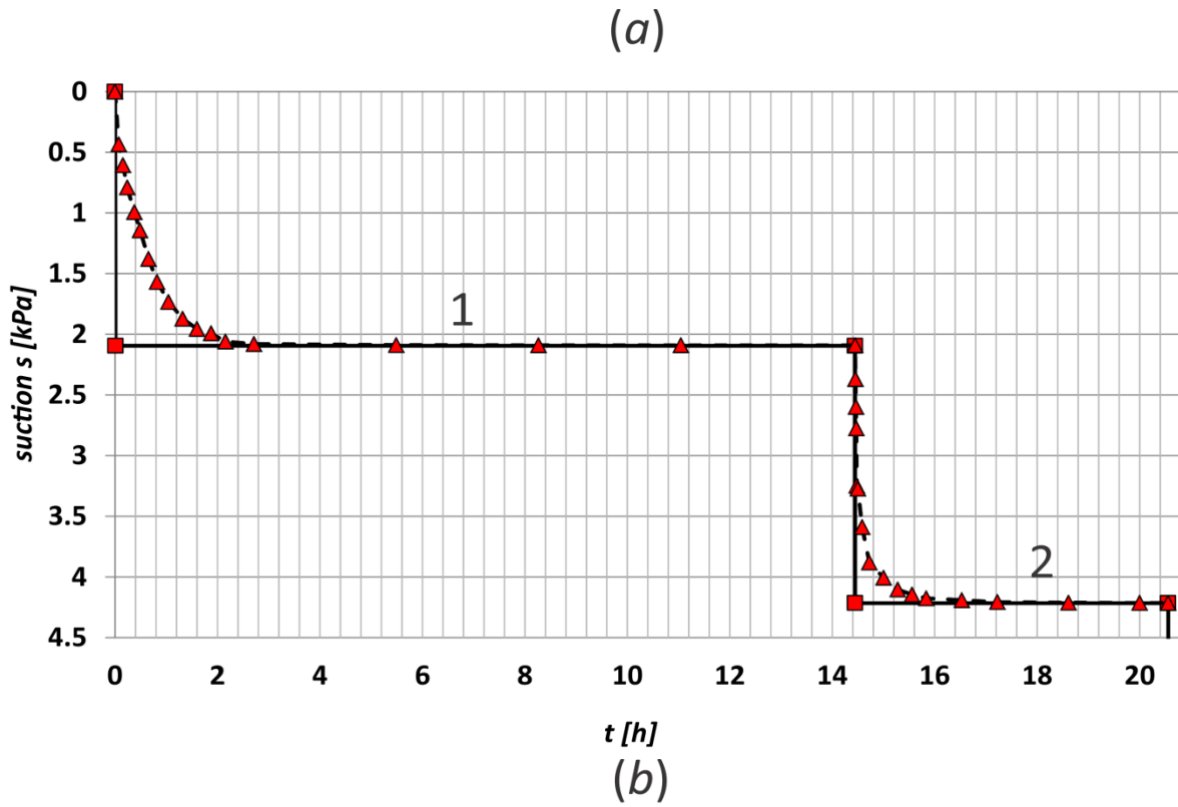
655

656

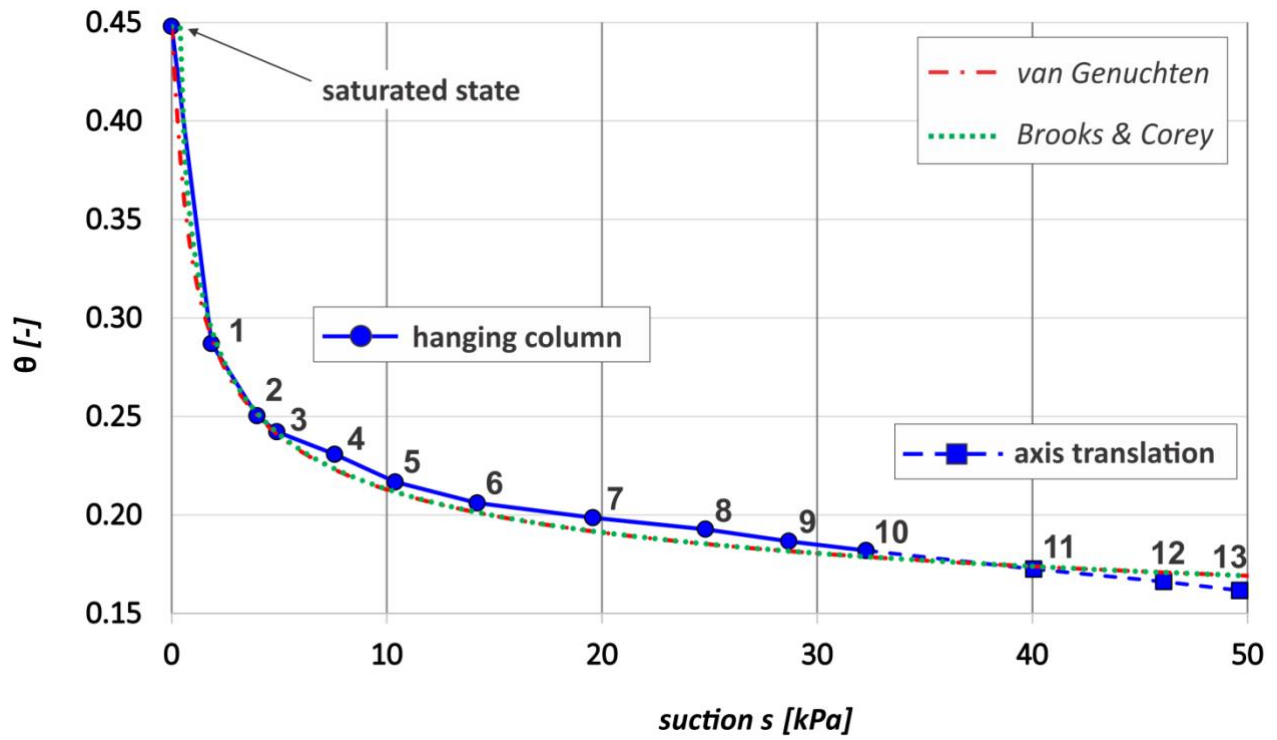
657

658

659



660
 661 *Figure 8. Zoom of the suction changes (solid line with rectangles – imposed suction; dashed line*
 662 *with triangles – calculated suction at the top of the ceramic disk): a) steps 1 and 2; b) steps 11 and*
 663



664

665 *Figure 9. Water retention curve obtained using both techniques of controlling suction (hanging*
 666 *column and axis translation)*

667

668

669

670

671

672

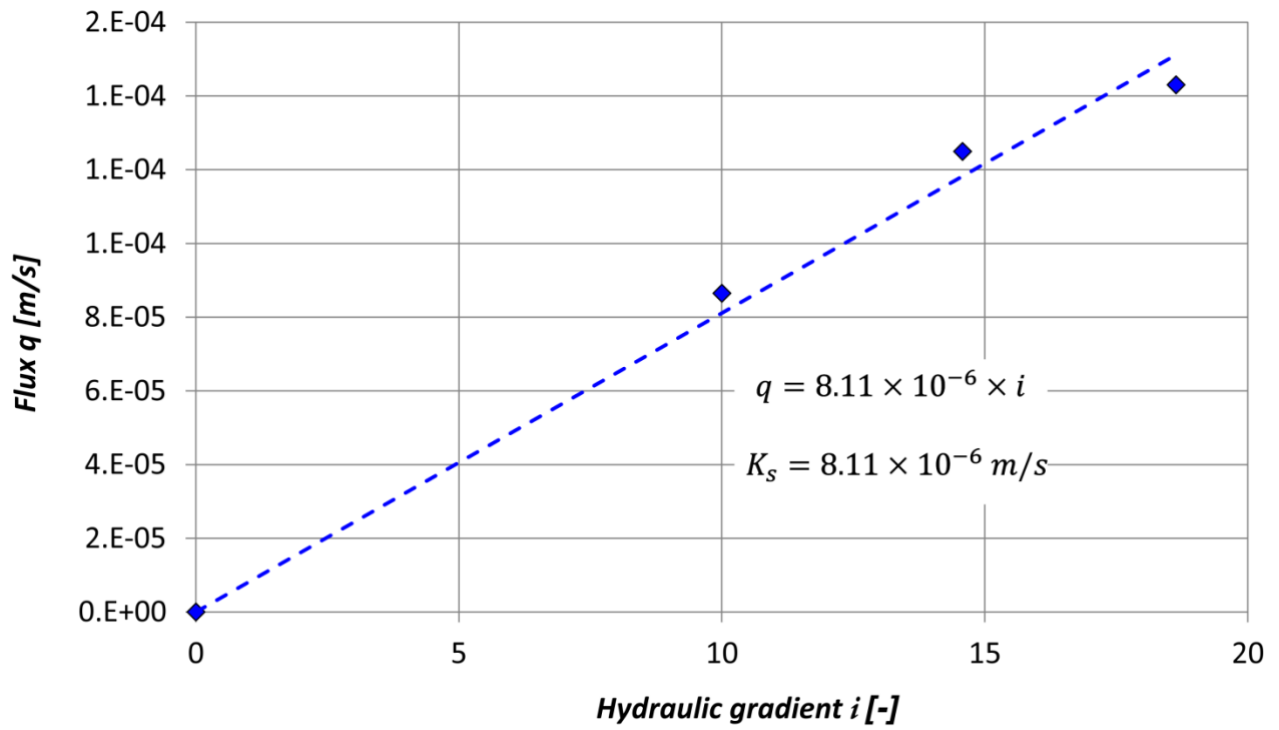
673

674

675

676

677



678

679 *Figure 10. Data of the constant water head hydraulic conductivity measurement of the saturated*
 680 *material.*

681

682

683

684

685

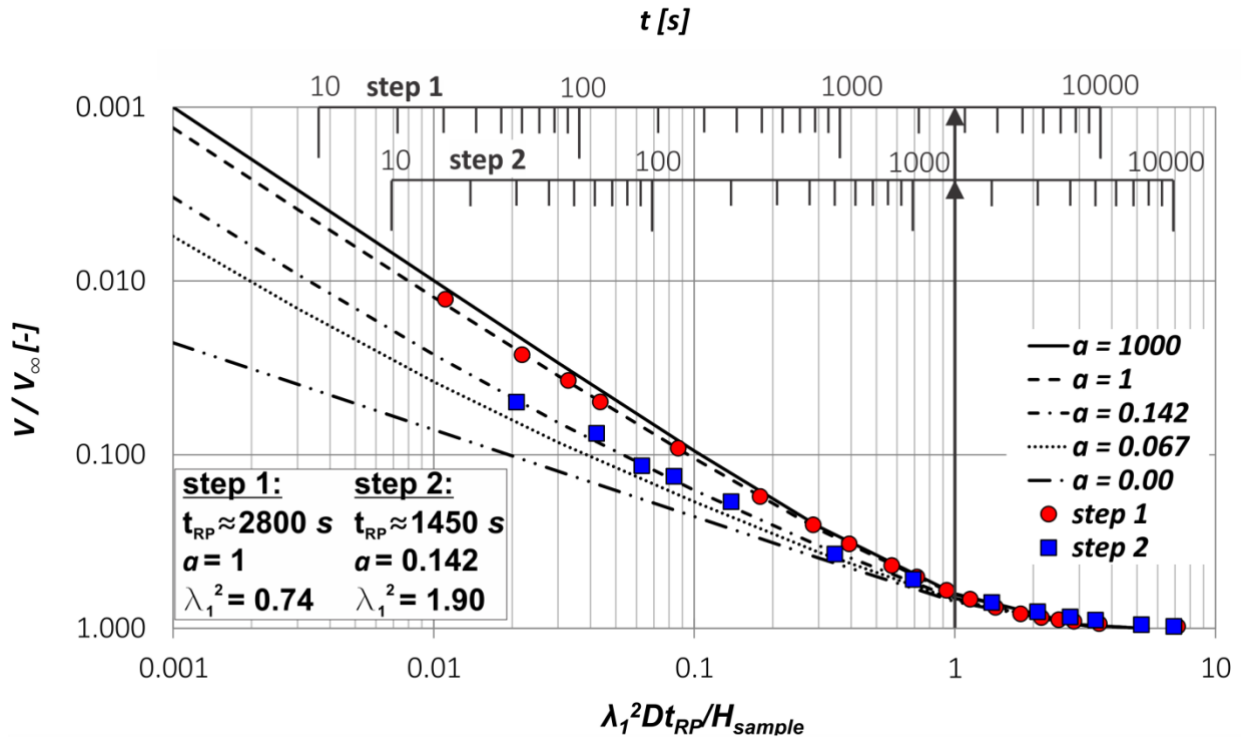
686

687

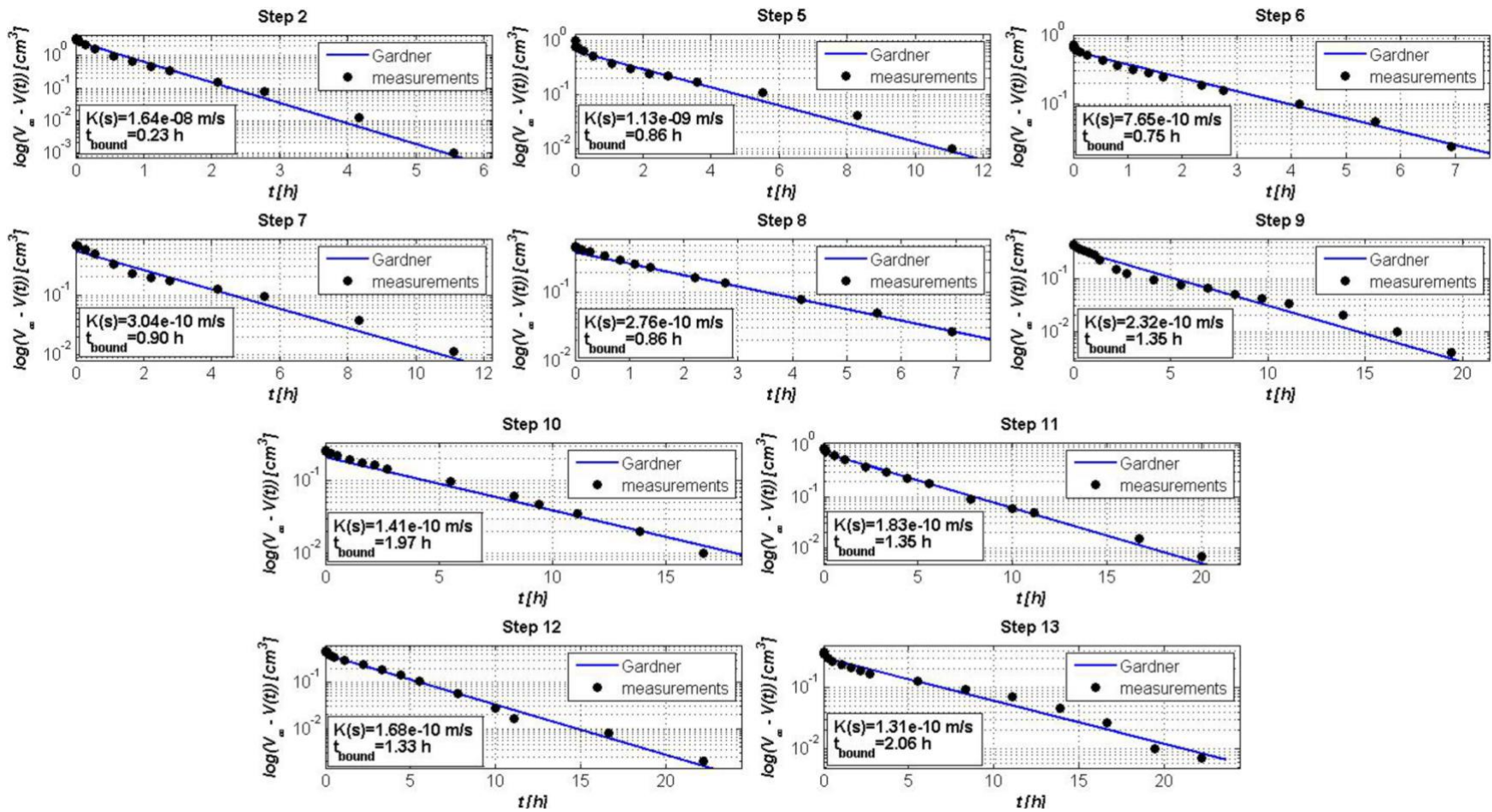
688

689

690



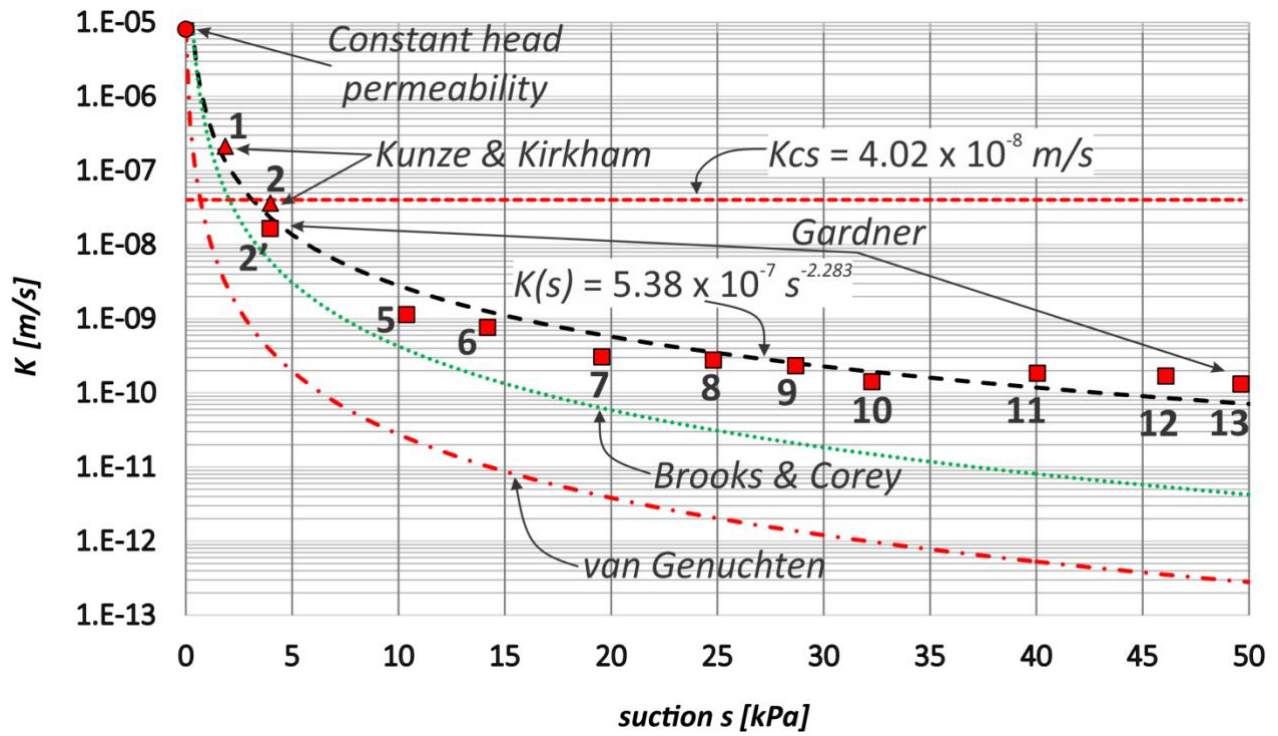
691
 692 *Figure 11. Kunze and Kirkham's method applied to measurements 1 and 2 (arrow indicates t_{RP})*
 693
 694
 695
 696



697

698 *Figure 12. Data from Gardner's method, suction steps 2 and 5 – 13*

699



700

701 *Figure 13. Hydraulic conductivity function (HCF)*

702